Bound-state instability of the chiral Luttinger liquid in one dimension

A. F. Ho* and P. Coleman

Serin Laboratory of Physics, Rutgers University, 136 Frelinghuysen Road, Piscataway, New Jersey 08854
(Received 21 January 2000)

We have developed a ''bootstrap'' method for solving a class of interacting one-dimensional chiral fermions. The conventional model for interacting right-moving electrons with spin has an SO(4) symmetry, and can be written as four interacting Majorana fermions, each with the same velocity. We have found a method for solving some cases when the velocities of these Majorana fermions are no longer equal. We demonstrate in some detail the remarkable result that corrections to the skeleton self-energy identically vanish for these models, and this enables us to solve them exactly. For the cases where the model can be solved by bosonization, our method can be explicitly checked. However, we are also able to solve some cases where the excitation spectrum differs qualitatively from a Luttinger liquid. Of particular interest is the so-called SO(3) model, where a triplet of Majorana fermions, moving at one velocity, interact with a single Majorana fermion moving at another velocity. Using our method we show, that a sharp bound (or antibound) state splits off from the original Luttinger-liquid continuum, cutting off the x-ray singularity to form a broad incoherent excitation with a lifetime that grows linearly with frequency.

I. INTRODUCTION

The anomalous normal-state behavior discovered in cuprate superconductors has stimulated enormous interest in the possibility of types of electronic fluid that might provide an alternative to Fermi-liquid behavior. The classic model for non-Fermi-liquid behavior is provided by the one-dimensional (1D) electron gas, where the generic fixed-point behavior is a Luttinger liquid.[1] Thanks to a wide array of nonperturbative techniques, there is a rather solid understanding of the non-Fermi-liquid properties in such 1D systems. Motivated by an early suggestion of Anderson,[2] many authors have attempted to generalize the Luttinger liquid concept to higher dimensions.[3–5]

The Luttinger liquid in one dimension is truly special in that it has no quasiparticle poles but a branch cut singularity; its correlation functions are scale invariant, with an associated beta function that is zero to all orders in perturbation theory[3] for a wide range in the coupling:

$$\beta(g)=0.$$

That the β function is zero is not in itself special to the Luttinger liquid. For example, in the absence of nesting, or a Cooper instability, the β function associated with Landau's Fermi-liquid fixed point is also zero for the forward scattering channel.[6,7]

The profound differences between the Luttinger-liquid and Landau-Fermi-liquid fixed points originate in the special kinematics of one dimension. In one dimension, the Fermi surface consists of just two points $\pm k_f$ where the electrons interact very strongly, and asymptotically near these Fermi points, energy and momentum conservation impose a *single* constraint on scattering processes, giving rise to a qualitative enhancement in scattering phase space. This causes the electron to lose its eigenstate status to the collective spin- and charge-density bosonic modes. Luttinger-liquid behavior requires the absence of umklapp interactions, and in this case,

left- and right-moving particles are separately conserved. The spin and charge current densities of the right- (or left-) moving particles are then simply proportional to the corresponding spin and charge densities:

$$J_c^R = v_c \rho_c^R,$$

$$J_s^R = v_s \rho_s^R,$$

so that the continuity equation assumes a special form

$$(\partial_\tau - i v_{s,c} \partial_x)\rho_{s,c}^R = 0.$$

As noted long ago by Dzyaloshinskii and Larkin[8] (also see Ref. 3), these conservation laws lead to the vanishing of the N-point connected current correlation functions for $N>2$ (''loop cancellation theorem''; see Sec. IV), which leads to a Gaussian theory for the spin and charge bosons in the Tomonaga Luttinger model, and also for the low energy effective theory of the Hubbard model in one dimension.

Unfortunately, the special kinematics of one dimension do not survive in higher dimensions, and largely for this reason, attempts to generalize the Luttinger liquid to $d \geq 2$ with strictly local interactions have been unsuccessful. In one dimension, energy and momentum conservation impose a single constraint on the forward-scattering processes, whereas, in higher dimensions, they impose independent constraints on the scattering processes. These additional constraints eliminate many of the potentially dangerous singularities present in one-dimensional scattering processes, stabilizing the Fermi liquid in two or higher dimensions.[3,7] Lin *et al.*[9] arrived at the same conclusion, making the passage from one to two dimensions by coupling N Hubbard chains together and taking the limit $N \to \infty$.[10] While it is possible to circumvent the Fermi liquid in two dimensions by introducing long-range or singular interactions,[11,12,2] a route to non-Fermi-liquid behavior in two dimensions that involves strictly local interactions has not yet been found.
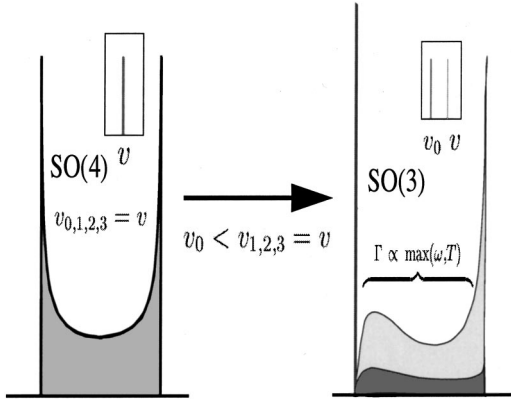
FIG. 1. Schematic diagram showing the evolution of the spectral weight as we introduce a velocity difference to the fermions. The inset indicates the bare spectral function, without interactions.

However, an alternative approach was advocated by Anderson,[13] who noted that higher-dimensional non-Fermi-liquid behavior might derive from the formation of bound or antibound states above and below the single-particle continuum. Such bound states play an important role in the formation of the one dimensional Luttinger liquid, where they give rise to a finite scattering phase shift at the Fermi energy, driving the formation of x-ray singularities in the spinon-holon continuum.

In this paper, we are motivated by this discussion to examine whether such singularities are robust against the removal of some of the special kinematic symmetries of one dimension. By modifying the 1D kinematics, we show that it is possible to actually split-off bound states from the spinon-holon continuum giving rise to a type of one-dimensional non-Fermi liquid that does not rely on the special 1D symmetries mentioned above. The key to our idea is as follows. The electron fluid on the Fermi surface is made up of spin-up and -down electrons and holes. Borrowing from the Dirac equation, we can rewrite the electrons and holes as charge-conjugation eigenstates,

$$c_\uparrow = \frac{1}{\sqrt{2}}(\Psi^{(1)} - i\Psi^{(2)}), \quad c_\downarrow = -\frac{1}{\sqrt{2}}(\Psi^{(3)} + i\Psi^{(0)}),$$

where $\Psi^{(a)}$ $[a=(0,1,2,3)]$ represent four chiral Majorana fermions[14] such that $\Psi^{(a)}(x) = \Psi^{(a)\dagger}(x)$. Instead of changing the interaction, we modify the scattering kinematics by making one of the Majorana fermions to have a different velocity to the others. In the classic Tomonaga Luttinger model, all four Majorana fermions have the same velocity [exhibiting the full SO(4) symmetry], and this leads to the special 1D kinematics mentioned above. But in our model [with the reduced SO(3) symmetry], lifting the velocity degeneracy causes the energy and momentum conservation to be distinct constraints in scattering phase space. We shall show that, in this case, the reduced (relative to the Luttinger model) scattering cuts off the x-ray catastrophe associated with the Luttinger-liquid behavior. The ''hornlike'' feature in the spectral weight of the Luttinger liquid is then split into a sharp bound (or antibound) state that coexists with an incoherent spin-charge decoupled continuum. We summarize these results in Fig. 1.
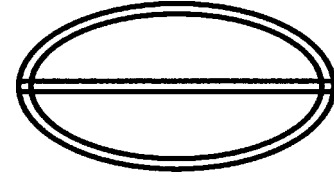

FIG. 2. Renormalized ''skeleton self-energy'' (SSE), where double lines represent full propagators.

While the main motivation of our model has been to find a fixed-point behavior in one dimension, our model [Eq. (3)] also has physical relevance to these recent work.

(i) The transport phenomenology of the cuprates[15] suggests that electrons near the Fermi surface might divide into two Majorana modes with different scattering rates and dispersion. To date, this kind of behavior has only been realized in impurity models[16] and their infinite-dimensional generalization.[17] We shall show that by breaking the velocity degeneracy of the original chiral Luttinger model, we obtain a one-dimensional realization of this behavior: a sharp Majorana mode intimately coexisting with an incoherent continuum of excitations, reminiscent of the higher-dimensional phenomenology.

(ii) Frahm et al.[18] proposed that the low-energy effective Hamiltonian of an integrable spin-1 Heisenberg chain doped with mobile spin-$\frac{1}{2}$ holes is given by Eq. (3), with one Majorana fermion $\Psi^{(0)}$ describing a slow moving excitation coming from the dopant, interacting with three rapidly moving Majorana fermions that describe the spin-1 excitations[19] of the spin-chain (see Sec. VI). Such doped spin-chain models may be relevant to certain experimental systems such as $Y_{2-x}Ca_x Ni O_5$.[20]

(iii) Recently Naud et al.[21] found that in a particular double-layer quantum Hall system with interlayer tunneling, the spectrum of the edge state consists of two Majorana fermions with different, dynamically generated, velocities. The class of models analyzed here may well be relevant to such multilayer, coupled quantum Hall systems.

Whereas the SO(4) model can be treated by bosonization,[1,22] by changing the velocity of a *single* Majorana fermion we introduce a nonlinear term into the bosonized Hamiltonian that preclude a separation in terms of Gaussian spin and charge bosons (see Sec. VI).

To tackle this SO(3) model, we have developed a fermionic ''bootstrap'' method, that has its basis the diagrammatic approach of Dzyaloshinskii and Larkin (1974).[8] Their method depends crucially on the existence of conserved currents to eliminate large sets of diagrams, leading to a closed set of equations that can be solved analytically for the Green function. On first glance, the reduced number of conserved currents in the SO(3) model [compared to the SO(4) model] causes the Dzyaloshinskii-Larkin method to be inapplicable, because one has to deal with nonconserved current vertices that involve the singlet Majorana fermion of different velocity. We have found, however, that by dealing directly with fermionic propagators and the four-leg fermionic vertex, bypassing the intermediate currents, there are enough conservation laws after all to eliminate all vertex corrections to the skeleton self-energy (Fig. 2), allowing us to write down a

compact set of coupled equations involving only the fully renormalized skeleton self-energy and the exact Green function of the theory.

The plan of the paper is as follows. In Sec. II, we define the class of models of interest here. In Sec. III, we describe our modification of the classic Dzyaloshinskii-Larkin[8] diagrammatic method for solving one-dimensional fermionic systems, to deal with our case where not all the velocities are the same. In Sec. IV, we take advantage of the purely chiral nature of our model (3) to write down a scaling form to simplify considerably the bootstrap equations derived in Sec. III. In Sec. V, we derive asymptotic solutions for frequencies near the spectral weight singularities, and demonstrate our results with numerical solutions. In Sec. VI, we discuss the nature of this new fixed point. Some of the results appeared in a brief form in Ref. 23.

II. MODEL

The class of model we study here is

$$H = \int dx \left\{ -i \sum_{a=0}^{3} v_a \Psi^{(a)}(x) \partial_x \Psi^{(a)}(x) \right.$$

$$\left. + g \Psi^{(0)}(x) \Psi^{(1)}(x) \Psi^{(2)}(x) \Psi^{(3)}(x) \right\}, \quad (1)$$

where $\Psi^{(a)}$ are real (Majorana) fermions such that $\Psi^{(a)}(x) = \Psi^{(a)\dagger}(x)$. The fermions are chiral (right movers, say): this is one crucial property that ensures that the system stays gapless, and allows for exact solutions in a number of cases.

In the special case where all velocities are the same, this model has an SO(4) symmetry, where the four Majorana modes can be associated with the spin-up and -down electron and hole excitations of the Fermi surface. To see this, write $c_\uparrow = (1/\sqrt{2})(\Psi^{(1)} - i\Psi^{(2)})$ and $c_\downarrow = -(1/\sqrt{2})(\Psi^{(3)} + i\Psi^{(0)})$, where c_α are the usual (chiral) Dirac fermions, and the SO(4) model is just the conventional one-branch spin-$\frac{1}{2}$ Luttinger model:

$$H_{SO(4)} = \int dx \left\{ \sum_{a,\sigma} c_\sigma^\dagger(x) i v \partial_x c_\sigma(x) + \text{H.c.} \right.$$

$$\left. - g[c_\uparrow^\dagger(x) c_\uparrow(x) - 1/2][c_\downarrow^\dagger(x) c_\downarrow(x) - 1/2] \right\}. \quad (2)$$

This SO(4) model can be shown by bosonization to be a Luttinger liquid.[22]

We shall mostly focus on the SO(3) model where $v_1 = v_2 = v_3 = v \neq v_0$:

$$H = \int dx \{ H_{kin}(x) + g \Psi^{(0)}(x) \Psi^{(1)}(x) \Psi^{(2)}(x) \Psi^{(3)}(x) \}, \quad (3)$$

$$H_{kin}(x) = -iv \sum_{a=1}^{3} \Psi^{(a)}(x) \partial_x \Psi^{(a)}(x)$$

$$- iv_0 \Psi^{(0)}(x) \partial_x \Psi^{(0)}(x).$$

Note that this model reduces to the single-impurity model of Coleman et al.[16] when the mode $\Psi^{(0)}$ is made to localize at the impurity site, and Ho and Coleman studied the same

lattice SO(3) model in high dimensions.[17] We will show that, by making the velocity of one Majorana fermion different, the scattering phase space decreases drastically, leading to this singlet splitting off from the Luttinger continuum to form a sharp bound-antibound state. Thus this is a system that has two qualitatively distinct relaxation rates, a dramatic departure from the Luttinger-liquid scenario.

The SO(2)×SO(2) model, where $v_0 = v_1 \neq v_2 = v_3$ is also solvable by bosonization, and interestingly, our bootstrap method also works here. (See Secs. V and VI.)

Finally, we shall also briefly look at the SO(2) model where $v_0 \neq v_1 \neq v_2 = v_3$. While we do not know if our method works here, we expect that due to the separate energy and momentum conservation, there is still a restriction of scattering phase space, and the theme of split-off sharp bound-antibound state continues. Note that the number of degrees of freedom and the interaction are the same in all the cases; the variety of behavior seen is due solely to changes in the scattering phase space, when the velocities of the fermions are made to be different.

III. METHOD—PHILOSOPHY

Our approach is based on the observation that for the SO(4) and SO(3) models (and possibly others too), the renormalized skeleton self-energy (SSE) containing full propagators, but no vertex corrections (Fig. 2) is *exact*, so that

$$\Sigma_a(x,\tau) = g^2 G_b(x,\tau) G_c(x,\tau) G_d(x,\tau), \quad (4)$$

where G_a are the exact, interacting Greens functions and $\{a,b,c,d\}$ is a cyclic permutation of $\{0,1,2,3\}$. These equations close with the usual relations

$$\Sigma_a(k,\omega) = (i\omega - v_a k) - G_a(k,\omega)^{-1} \quad (a=0,1,2,3). \quad (5)$$

Equations (4) and (5) together define a bootstrap method to solve the problem.

To show that there are no vertex corrections to the renormalized skeleton self-energy, we first review and then extend Dzyaloshinskii and Larkin's method. Provided that we have a minimal SO(3) symmetry, then the three current densities $j^a(x) = -i \epsilon_{abc} \Psi^{(b)}(x) \Psi^{(c)}(x)$ $[a,b,c \in (1,2,3)]$ are conserved classically. Following Dzyaloshinskii and Larkin,[8,3,24] since charge and current are proportional in a chiral model, the continuity equation guarantees that the N-point connected current-current correlation functions vanish for $N>2$ [$\mathbf{x}_i = (x_i, \tau_i)$]:

$$\langle j^a(\mathbf{x}_1) j^a(\mathbf{x}_2) \cdots j^a(\mathbf{x}_N) \rangle_C = 0 \quad (N>2). \quad (6)$$

For the noninteracting system, this result leads to the "loop cancellation theorem": for the amplitude associated with a closed fermion loop with $N>2$ conserved current insertions, the sum over all possible permutations of $\{\mathbf{x}_i\}$ of the current operators must give zero.[8,3,24] In Appendix A, for illustration, we give a derivation for the $N=4$ case and also for odd N. Dzyaloshinskii and Larkin used this cancellation to eliminate all diagrams that contain such closed loops, considerably simplifying the vertex function and polarization bubbles.

We use the loop cancellation theorem in a new way, to our knowledge, to show that the vertex corrections to the
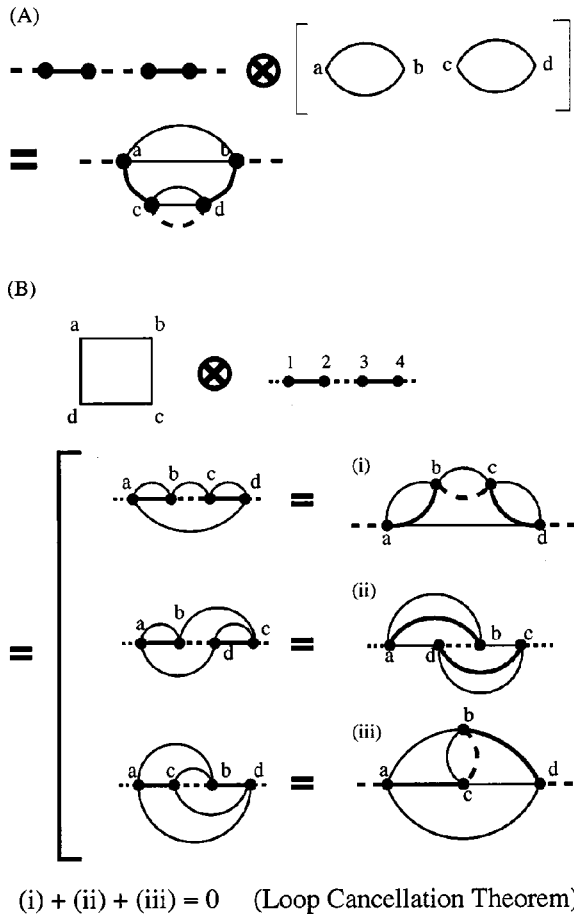
(A)

(B)

(i) + (ii) + (iii) = 0   (Loop Cancellation Theorem)

FIG. 3. (A) Illustrating how the only nonvanishing singlet self-energy at order g^4 is constructed by combining a propagator backbone with loops containing two vertex insertions. Dotted lines indicate a bare propagator for the singlet Majorana fermion $\Psi^{(0)}$. Full lines indicate a bare propagator for the triplet Majorana fermions. (B) Illustrating how the nonskeleton self-energy at order g^4 is constructed by combining a propagator backbone with loops containing four vertex insertions.

FIG. 4. List of all classes of free-energy diagrams that generate non-SSE diagrams at order g^6.

SSE (Fig. 2) identically vanish. Unlike Dzyaloshinskii and Larkin,[8,3,24] we discard the intermediate currents and the associated current vertices, and deal only with fermionic propagators and the four-leg interaction vertex. The loop cancellation theorem is the same. This method has the advantage that it is more compact (only the self-energy and the Green functions are involved), and treats all propagators in a symmetric manner. To illustrate the idea, consider the self-energy of the singlet Majorana mode in the SO(3) model. Figure 3 lists all such diagrams at order g^4. The Feynman diagrams contributing to the skeleton self-energy are constructed by combining loops with two insertions. This is clearly true for the second-order diagram, and we illustrate this using the first nontrivial order, the fourth-order diagram in Fig. 3(A), which holds to all orders in perturbation theory. Nonskeleton contributions to the self-energy involve diagrams with loops containing more than two current insertions. In these diagrams, the sum over all permutations of the current insertions into the loops is automatically zero, as illustrated to order g^4 in Fig. 3(B). A convenient way to represent these diagrams is to split each diagram into a backbone which is the same in all three diagrams, and the four-
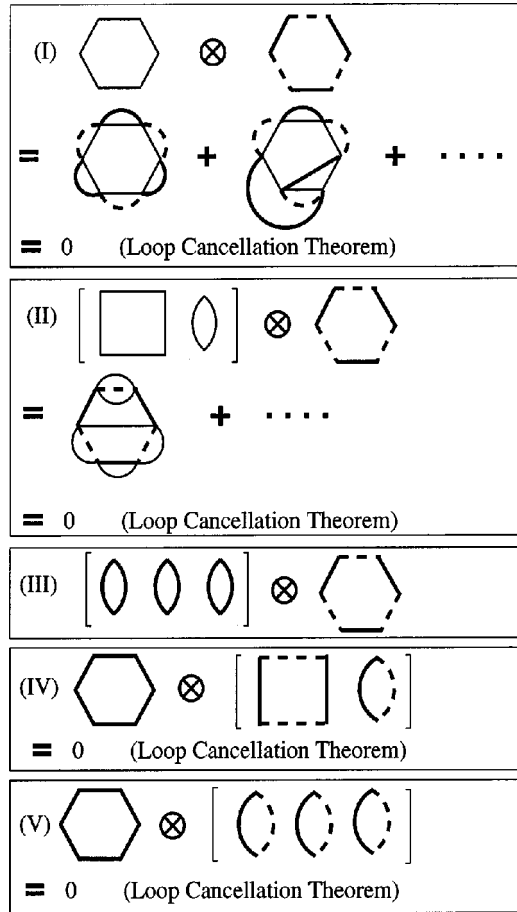
insertion loop. Inserting the four vertices of the four-loop construction in various ways into the four vertices of the backbone gives the three diagrams in Fig. 3(B). Note that this method of generating the diagrams give rise to the correct degeneracy for each of the diagram types $[(i)$, (ii), and $(iii)]$.

To generalize these results to higher-order graphs, it is more convenient to look at the set of diagrams for the free energy. Cutting a $\Psi^{(0)}$ line gives back the singlet self-energy Σ_0. We first note that only even orders in g occur in the free-energy expansion, because the bare Majorana propagators are diagonal in the Majorana flavor index. Next, there is always a closed loop with n propagators (not necessary of the same type) in any of the free-energy diagrams of order g^n. Otherwise, improper and/or disconnected self-energy diagrams would be generated. Then, at order g^6 for example, we have the following classes of diagrams listed in Fig. 4 that might generate non-SSE diagrams.

The loop cancellation theorem applies to each case where there is a closed loop with more than two propagators of the same kind. Thus case (iii) is the only one left. Yet, case (iii) generates either SSE diagrams, improper self-energy diagrams (where cutting one of the lines lead to two disconnected parts), or else diagrams that have already been counted in the other cases. The last observation follows from the fact one can always find a closed six- or four-loop construction buried in the diagram. Hence, all potential non-SSE generating diagrams disappear. One can clearly generalize
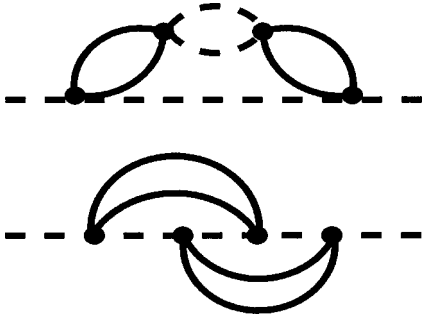
FIG. 5. Examples of nonskeleton self-energy diagrams in the $SO(2) \times SO(2)$ model, where the loop cancellation theorem does not apply.

the same reasoning to higher-order diagrams. We only need to check that this method deals with the combinatoric factors correctly, i.e., all the degeneracies of the diagrams are such that there are no non-SSE diagrams left over. Here we appeal to the fact that in the SO(4) model, there must also be the correct loop cancellations, because our method gives the same exact answer as Dzyaloshinskii and Larkin's method. Even though we have drawn the diagrams treating the triplet lines as identical, these triplet lines actually must carry a Majorana flavor index; to generate all possible diagrams whether distinct under SO(3) or not, we must draw all possible diagrams with proper indexing of each of the lines. Listing all diagrams this way is independent of which symmetry we are dealing with, and consequently, combinator factors will automatically be taken care of in performing loop cancellations with these Majorana indices on the propagator lines. In particular, the symmetry or combinatoric factors for each diagram must be just right to allow loop cancellation to work in the SO(4) case, and hence for the SO(3) case too.

Thus we can show that the vertex corrections to the self-energy Σ_0 of the singlet Majorana fermion cancel to all orders, leaving the fully renormalized SSE as the only remaining contribution. Intriguingly, this argument fails for the $SO(2) \times SO(2)$ model, because each vertex has two ''fast'' legs and two ''slow'' legs, unlike in the SO(3) case where there is only one of the singlet legs. Thus, for example, the non-SSE diagrams in Fig. 5 do not have a closed loop of only one kind of propagator, which would allow loop cancellation to apply. However, these diagrams cannot contribute to the exact self-energy either, because the $SO(2) \times SO(2)$ model can be solved exactly by bosonization, or by a slight extension of Dzyaloshinskii and Larkin's method, and these results agree exactly with our bootstrap method (see Sec. V). There must then be more cancellation than that due just to the loop cancellation theorem in its current form.

To complete our proof, we need to show that the triplet Majorana self-energy is also given by the skeleton diagram. We use the *full* Kadanoff-Baym free-energy functional

$$F[G] = -T\{\text{Tr} \ln[G^{-1}] + \text{Tr}[\Sigma G]\} + Y[G], \quad (7)$$

where $Y[G]$ is the sum of all skeleton diagrams.[25] Now, by construction, $\delta F[G]/\delta G_a = 0$ generates the equations for the self-energies, and in particular, $\delta F[G]/\delta G_0$ must generate the skeleton self-energy Σ_0. This requires that the Kadanoff-

Baym free-energy functional *truncates* at the leading skeleton diagram

$$F = -T\{\text{Tr} \ln[G^{-1}] + \text{Tr}[\Sigma G]\} + \text{⬭} \quad (8)$$

Finally, by differentiating the free-energy functional with respect to the exact Greens functions $G_{1,2,3}$ of the triplet Majorana fermions, each triplet self-energy is also given by the corresponding skeleton self-energy.

IV. METHOD—DETAILS

We now apply this result, using the limiting case of the SO(4) model to check the validity of our results. Our equations are dramatically simplified by seeking solutions to Eq. (4) which satisfy a scaling form

$$G_a(x,\tau) = \frac{1}{2\pi i x} \mathcal{G}_a(\tau/ix). \quad (9)$$

This form is motivated by the observation that chirality prevents space from acquiring an anomalous dimension, when the interaction is marginal (in the renormalization-group sense). Under a Fourier transform, this scaling form is self-dual,

$$\frac{1}{2\pi i x} \mathcal{G}_a(\tau/ix) \overset{F.T.}{\leftrightarrow} \frac{1}{i\omega} \mathcal{G}_a(k/i\omega), \quad (10)$$

where the *same* function $\mathcal{G}_a$ appears on both sides. Inserting Eq. (10) into Eq. (5) and Fourier transforming,

$$\Sigma_a(x,\tau) = -\frac{1}{2\pi(ix)^3} \frac{d^2}{du^2} [1 - v_a u - 1/\mathcal{G}_a(u)]_{u=\tau/ix}. \quad (11)$$

Since the bare Green function scaling form is $1/\mathcal{G}_a^0(u) = 1 - v_a u$, it does not contribute to the self-energy. Combining Eqs. (4) and (11),

$$\frac{d^2}{du^2} [\mathcal{G}_a(u)]^{-1} = -(g/2\pi)^2 \mathcal{G}_b(u)\mathcal{G}_c(u)\mathcal{G}_d(u), \quad (12)$$

where $\{a,b,c,d\}$ are cyclic permutations of $\{0,1,2,3\}$. The boundary conditions are

$$\mathcal{G}_a(0) = 1, \quad \mathcal{G}_a'(0) = v_a, \quad (13)$$

derived from the physical requirement that, at high frequencies, the fermions are free particles, moving with the *bare* velocity v_a. Equations (12) and (13) are the scaling form version of our bootstrap method [Eqs. (4) and (5)]. Note that the differential Eq. (12), like Eq. (4), is independent of the sign of the coupling g. Also, Eq. (12) has no information on which model of the class [Eq. (1)] it refers to; the symmetry of the model (i.e., the velocities) only comes in through boundary conditions (13).

For the SO(4) model, where $\mathcal{G}_a(u) \equiv \mathcal{G}(u)$ ($a = 0, \ldots, 3$), Eqs. (12) reduce to a single differential equation
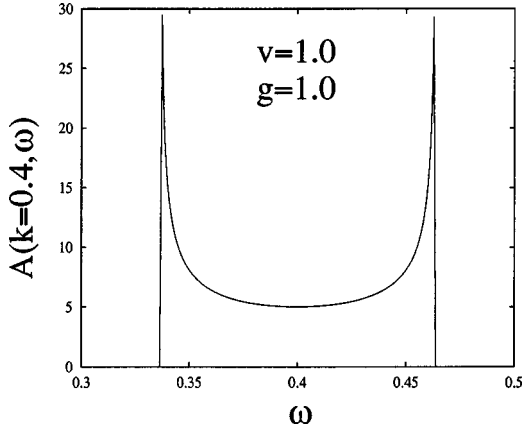
FIG. 6. Spectral weight of SO(4) model.

$$\frac{d^2}{du^2}[\mathcal{G}(u)]^{-1} = -(g/2\pi)^2[\mathcal{G}(u)]^3, \tag{14}$$

for which the solution satisfying the boundary conditions $\mathcal{G}(0) = 1$, and $\mathcal{G}'(0) = v$ is

$$G(x,\tau) = \frac{1}{2\pi ix}[1 - v_+ \tau/ix]^{-1/2}[1 - v_- \tau/ix]^{-1/2}, \tag{15}$$

where $v_\pm = v \pm (g/2\pi)$ and v is the bare velocity. Identical results are obtained by bosonization,[22] where v_+ and v_- are in fact the velocity of the spin boson and the charge boson. Thus this confirms that the skeleton self-energy is exact for the Luttinger model.

V. RESULTS

In the SO(4) model, the electron spectral weight displays two classic x-ray singularities associated with the decay of the electron into a spinon and holon continuum (Fig. 6).[22] We now show that if $\Delta v = v - v_0$ is finite, one of these x-ray edge singularities is completely eliminated. If $v_0 < v$, we find that the low-velocity "horn," originally with velocity v_-, develops a sharp bound-state pole in the singlet channel, and a broad incoherent excitation in the triplet channel with a lifetime growing linearly in energy. If $v_0 > v$, the high-velocity horn splits off a singlet antibound state, and the triplet channel develops a high-velocity incoherent excita-
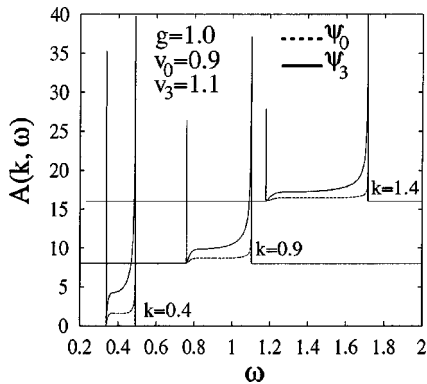

FIG. 7. Spectral weight of the SO(3) model. For clarity, we have shifted up the curves for various momenta by eight units.

tion. (Fig. 7). A sharp bound state in the singlet channel develops once a velocity difference is introduced, because energy and momentum conservation now provide distinct constraints to scattering [unlike in the SO(4) model], leading to much less phase space for $\Psi^{(0)}$ to decay into.

To see this, we must analyze Eq. (12) for the SO(3) case:

$$\frac{d^2}{du^2}\mathcal{G}_3^{-1} = -(g/2\pi)^2(\mathcal{G}_3)^2\mathcal{G}_0,$$
$$\tag{16}$$
$$\frac{d^2}{du^2}\mathcal{G}_0^{-1} = -(g/2\pi)^2(\mathcal{G}_3)^3.$$

A very convenient way to discuss these equations is to map them onto a central force problem. If we write $\mathbf{r} = (\mathcal{G}_3^{-1}, \mathcal{G}_0^{-1})$ and $\mathbf{F} = -(g\mathcal{G}_3/2\pi)^2(\mathcal{G}_0, \mathcal{G}_3)$, then, $\ddot{\mathbf{r}} = \mathbf{F}$, where $\ddot{\mathbf{r}} \equiv d^2\mathbf{r}/du^2$, i.e., u is like "time." By inspection, $\mathbf{r} \times \mathbf{F} = 0$, so the force is radial, thus the "angular momentum," $\mathbf{r} \times \dot{\mathbf{r}} = \Delta v$ is a constant. If we use polar coordinates, $(\mathcal{G}_3^{-1}, \mathcal{G}_0^{-1}) = r(\cos\theta, \sin\theta)$ the equations for the Green function resemble the motion of a fictitious particle under the influence of an anisotropic central force:

$$\ddot{r} - \frac{\Delta v^2}{r^3} = -(g/2\pi)^2\frac{1}{r^3\cos^3\theta\sin\theta},$$
$$\tag{17}$$
$$r^2\dot{\theta} = \Delta v.$$

The velocity difference $\Delta v = v - v_0$ provides a repulsive centrifugal force. The boundary conditions (13) mean that the "particle" starts out at $r(0) = \sqrt{2}, \theta(0) = \pi/4$, and with a slope change $\dot{\theta}(0) = \Delta v/2$.

Without loss of generality, let $\Delta v \leq 0$. For $\Delta v > 0$ simply replace $v_+ \rightarrow v_-$ and $g \rightarrow -g$. When $\Delta v = 0$, the "particle" falls directly into the origin, and both $\mathcal{G}_3$ and $\mathcal{G}_0$ diverge with x-ray singularities when the particle first hit the origin at "time" $u = 1/v_+$. Then the particle goes purely imaginary in both coordinates, which gives rise to the Luttinger continuum in the spectral weight, until the time $u = 1/v_-$ when the particle goes back to the origin, leading to the other x-ray singularities for both $\mathcal{G}_3$ and $\mathcal{G}_0$. From then on, the particle stays in the real plane (Fig. 9).

However, once $\Delta v < 0$ is finite, $\dot{\theta}(0) = \Delta v$ causes the orbit to miss the origin at $u \sim 1/v_+$. Instead, $\theta \rightarrow 0$ at some finite "time" $u = 1/v_0^*$ (Fig. 8), at which $r = C$ and $\dot{\theta} = \Delta v/C^2$. For $u \sim 1/v_0^*$, it follows that $(r, \theta) = [C, \dot{\theta}(u - 1/v_0^*)]$, from which we can read off the following asymptotics:

$$\mathcal{G}_3(u)^{-1} \sim C, \tag{18}$$

$$\mathcal{G}_0(u)^{-1} \sim (1 - uv_0^*)/Z, \quad Z = Cv_0^*/|\Delta v|. \tag{19}$$

Thus the associated x-ray singularity in the spectral function for both $\mathcal{G}_3$ and $\mathcal{G}_0$ is eliminated, replaced by an antibound state for the singlet $\mathcal{G}_0$ with spectral weight Z, moving with velocity v_0^*, splitting off above the continuum. After this time, $\mathbf{r}$ is complex in both coordinates, until eventually, at
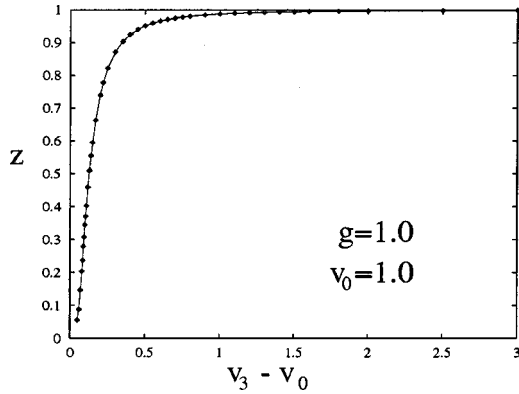
FIG. 8. Quasiparticle weight Z of $\Psi^{(0)}$ in the SO(3) model.

$u = 1/v_3^*$, the particle passes through the origin, giving rise to the remaining x-ray singularity at $u = 1/v_3^*$ in both $\mathcal{G}_3$ and $\mathcal{G}_0$.

The quantity $\zeta = (v - v_0)/g$ plays the role of a coupling constant, and approximate analytic solutions are possible in the limiting cases of small and large ζ. For $|\Delta v| \gg |g|/2\pi$ interactions can be ignored, so $v_0^* \to v_0$, and $Z \to 1^-$. For $|\Delta v| \ll |g|/2\pi$, the ''motion'' of the fictitious particle emulates that of the SO(4) model until the angle θ approaches zero. We may estimate v_0^* and C by integrating Eq. (17) with the approximation $r(u) \approx \tilde{r}(u)$, where $\tilde{r} = [2(1-v_+u)(1-v_-u)]^{1/2}$ is the SO(4) solution:

$$\int_0^{1/v_0^*} \frac{d\theta}{du} du = -\frac{\pi}{4} = \int_0^{1/v_0^*} \frac{\Delta v}{\tilde{r}^2(u)} du,$$

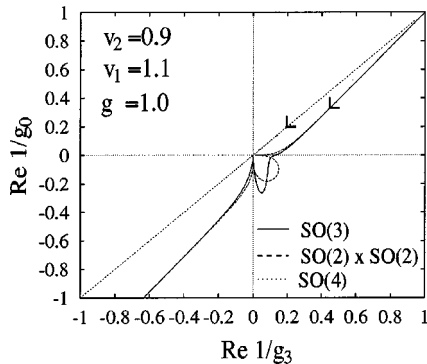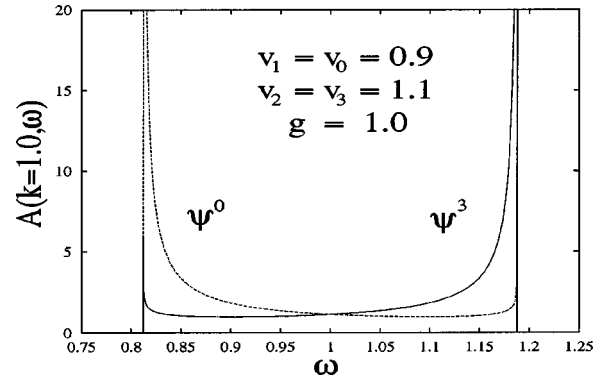$$C \approx \tilde{r}(1/v_0^*). \tag{20}$$

After doing the integral, this estimate gives (for $|\Delta v| \ll |g|/2\pi$)

$$v_0^* = v_+ + \frac{g}{\pi} \exp - \left| \frac{g}{2\Delta v} \right|, \tag{21}$$

$$Z = \left| \frac{\sqrt{2}g}{\pi \Delta v} \right| \exp - \left| \frac{g}{4\Delta v} \right|, \tag{22}$$

indicating that the formation of the sharp antibound state is nonperturbative in the velocity difference.

FIG. 9. ''Trajectory'' in the (Re $1/\mathcal{G}_3$, Re $1/\mathcal{G}_0$) plane. The arrows indicate the direction of increasing ''time'' u.

FIG. 10. Spectral weight of the SO(2)×SO(2) model.

To illustrate these results further, we have carried out numerical solutions of the differential equations (16) for intermediate values of the coupling constant ζ, using a standard adaptive integration routine.[26] Results are summarized in Figs. 7 and 8.

While we have not established the validity of our method to models of lower symmetry (but see Sec. VI), we believe that the method captures the essence of the kinematic constraints imposed by energy and momentum conservation, at least for weak coupling. Thus we have also performed numerical calculations for the SO(2)×SO(2) and SO(2) models.

For the SO(2)×SO(2) model, the pair $\Psi^{(0)}$ and $\Psi^{(1)}$ with the same bare velocity can combine together to form a boson, and similarly for $\Psi^{(2)}$ and $\Psi^{(3)}$. This leads back to a Luttinger-liquid form, but with asymmetric power-law singularities at the renormalized velocities v_+ and v_- (Fig. 10). [Also see Eq. (29) in Sec. VI, for an exact analytical solution for this model.]

As we progress to the SO(2) case, when $v_0 < v_1 = v_2 < v_3$, we see a sharp pole for the fermion which has an extremal velocity different to all the others, while the Luttinger continuum turns into wide peaks linear in energy for the fermion(s) with intermediate velocities; see Fig. 11. This illustrates once more our contention that making one Majorana degree of freedom to have a different (extremal) velocity causes drastic collapse of the scattering phase space for this fermion.
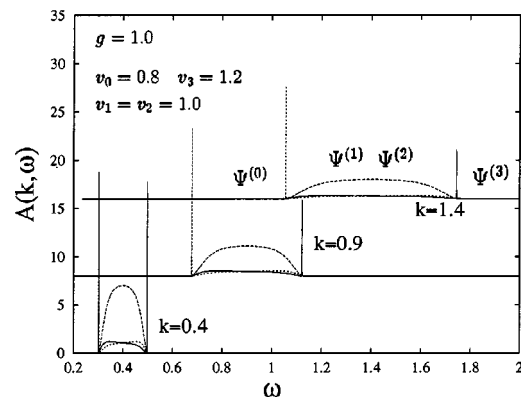

FIG. 11. Spectral weight of the SO(2) model. For clarity, we have shifted up the curves for various momenta by eight units.

VI. DISCUSSION AND CONCLUSION

A. 1D Majorana SO(3) model

In summary, we have demonstrated that by breaking the velocity degeneracy of a system of interacting chiral fermions we restrict the scattering phase space in a way that causes a sharp bound state or antibound state to split off from the spin-charge continuum, leading to a system with two qualitatively distinct spectral peaks and scattering rates. This is a significant departure from the Luttinger-liquid scenario, and demonstrates an interesting class of one-dimensional fixed-point behavior.

This fixed-point exhibits properties in common with both Luttinger and Fermi liquids, and is perhaps closest in character to the marginal Fermi-liquid phenomenology introduced in the context of cuprate metals.[27] Like the Fermi liquid, there is a sharp quasiparticle bound state, but this coexists with a Luttinger-liquid-like continuum which is bounded by two extremal velocities.

As mentioned, the SO(3) model does not appear to be solvable by conventional bosonization, forcing us to introduce this bootstrap method. Two immediate questions arise: the nature of the SO(3) fixed point, and the range of validity of the bootstrap method.

In the SO(4) model, the fermionic spectral weight has x-ray singularities at the velocities v_+ and v_- (see Sec. IV). By bosonization, the model can be mapped onto a theory of *free* bosons (the spin boson and charge boson) moving at v_+ and v_-, where for $g>0$, $v_{spin}=v_-$ and $v_{charge}=v_+$, and for $g<0$, the role of v_+ and v_- are exchanged. This is a direct consequence of separate charge and spin conservation in the model.[3] We can demonstrate this in the Majorana fermionic representation. The classically conserved densities are

$$J_{01}(x) \equiv -i\Psi^{(0)}(x)\Psi^{(1)}(x),$$
$$J_{23}(x) \equiv -i\Psi^{(2)}(x)\Psi^{(3)}(x). \tag{23}$$

[By the SO(4) symmetry, we can also define other combinations.] Using the commutation relations listed in Appendix B, we obtain the equations of motion

$$(-\partial_\tau - vq)J_{01}(q) = \frac{g}{2\pi}qJ_{23}(q),$$
$$(-\partial_\tau - vq)J_{23}(q) = \frac{g}{2\pi}qJ_{01}(q). \tag{24}$$

The right-hand side of the equations is not zero (as would be expected for conserved currents) because of the anomalous commutator (Appendix B),

$$[J_{01}(p), J_{01}(q)] = [J_{23}(p), J_{23}(q)] = p\delta(p+q), \tag{25}$$

which is the SU(2) level-2 Kac-Moody algebra anomaly.[30] Fortunately, by diagonalizing system (24), the linear combinations $J_-(q) = J_{01}(q) - J_{23}(q)$ and $J_+(q) = J_{01}(q) + J_{23}(q)$ do satisfy the continuity equations

$$(-\partial_\tau - v_+ q)J_+(q) = 0,$$
$$(-\partial_\tau - v_- q)J_-(q) = 0, \tag{26}$$

where $v_\pm$ is as before in Eq. (15), indicating that these densities $J_\pm$ are proportional to the spin boson and the charge boson.[31] This then leads to sharp poles in the charge and spin susceptibilities.

For the SO(3) model, using the same definitions [Eq. (23)], we find

$$(-\partial_\tau - v_0 q)J_{01}(q) = \frac{g}{2\pi}qJ_{23}(q) + (v_3 - v_0)K_{01}(q), \tag{27}$$

$$(-\partial_\tau - v_3 q)J_{23}(q) = \frac{g}{2\pi}qJ_{01}(q),$$

where $K_{01}(q) \equiv -i\Sigma_k k\Psi^{(0)}(q-k)\Psi^{(1)}(k)$. This extra term comes from the commutator of J_{01} and the kinetic energy, and causes the set of equations (27) not to close, and bosonization in terms of free spin and charge-bosons (or any linear combinations) is impossible. In short, because of the anomaly, the classically conserved SO(3) density J_{23} is admixed with the classically nonconserved J_{01}, leading to the loss of a sharp pole for the susceptibility corresponding to J_{23}. This makes it very different to the conformally invariant fixed points of the SO(4) model and the SO(2)×SO(2) model (see below). Also, the presence of a sharp pole in the fermionic spectral weight indicates that there is at least one (Majorana) fermionic degree of freedom in the diagonalized system.

Frahm *et al.*[18] has conjectured that this SO(3) model is the low-energy effective theory of an integrable model of a spin-1 chain doped with spin-$\frac{1}{2}$ mobile holes. Using the thermodynamic Bethe ansatz, they showed that the spin and charge sectors of the doped holes become decoupled at low temperatures, and they calculated the low temperature free energy of the spin contribution to be

$$F_{spin} = -\frac{\pi T^2}{6v_0}\left(\frac{1}{2} - \frac{3A}{4\pi}\ln A\right) - \frac{\pi T^2}{6v}\left(\frac{3}{2} + \frac{3A}{4\pi}\ln A\right) + \cdots, \tag{28}$$

where $A>0$ is a constant that depends on the doping only. With $A=0$ (undoped case), the first term has been interpreted[18] as coming from a single Majorana fermion of velocity v_0, and the second term from a triplet of massless Majorana fermions with velocity v that represent the SU(2) level-2 WZNW model, which was shown by Affleck[19] to be the low-energy effective theory of the gapless integrable spin-1 chain. Here a system of fermions with two velocities cannot be conformally invariant, unless the two species do not interact with each other and thus form two decoupled sectors that are *individually* conformally invariant.[32] Thus this is unlikely to be a conformal field theory. However, the form of the free energy [Eq. (28)] suggests that the SO(3) model is again asymptotically scale invariant, and we have found the coupling of the SO(3) model to be marginal, at least up to $O(g^3)$.[33]

As for the range of validity of the bootstrap method we introduced to solve the model, we note that if we change two Majorana velocities at the same time, so that $v_0 = v_1$ and $v_2 = v_3$, we would have reduced the symmetry still further, to an SO(2)×SO(2) symmetry.[28] We can solve the differential equations (12) with the results

$$G_3(x,\tau) = \frac{1}{2\pi i x}\left[1 - \frac{v_+\tau}{ix}\right]^{-(1/2)+\gamma}\left[1 - \frac{v_-\tau}{ix}\right]^{-(1/2)-\gamma},$$

(29)

$$v_\pm = \frac{1}{2}\{v_0 + v_3 \pm [(v_3 - v_0)^2 + (g/\pi)^2]^{1/2}\},$$

and $\gamma = \frac{1}{2}(v_3 - v_0)\{(v_3 - v_0)^2 + (g/\pi)^2\}^{-1/2}$. Interestingly, this model can be bosonized to a model of free bosons, and the bosonization result agrees exactly with Eq. (29). This is surprising because, as far as we can see, the closed-loop cancellation is not sufficient in the case of the $SO(2) \times SO(2)$ model to cancel all vertex corrections. This suggests that a more general cancellation principle is at work, and that the range of validity of our solution may even extend to models with a still smaller, $SO(2)$, symmetry. To date, we have not been able to prove this result.

We also wish to point out that our differential version [Eq. (12)] of the bootstrap equations (4) and (5) are of such a simple form only because we have a purely chiral system. If we allow left and right movers to interact, the scaling form [Eq. (9)] no longer applies,[22] and we have not found a different scaling form that allows similar simplifications. However, we expect the bootstrap method still to work, as long as there are separate conservation of left and right currents. This is true at least for the $SO(4)$ model, because Dzyaloshinskii and Larkin[8] showed that their method also works for such systems, and our method is a generalization of theirs.

B. Broader issues: Higher dimensions?

Our work raises the question whether this kind of non-Fermi-liquid behavior might survive in dimensions higher than one (Fig. 12). In higher dimensions energy conservation and momentum conservation are distinct constraints on scattering phase space, and the Luttinger liquid reverts to a Fermi liquid, at least for short-range interactions.[3,7] In contrast, the $SO(3)$ model does not appear to be solvable by bosonization, and its unusual properties have reduced reliance on the special kinematics in one dimension. Thus, this kind of behavior might be more robust in higher dimensions. In fact, near infinite dimensions,[17] two lifetimes of behavior persist in the $SO(3)$ model, but here, the thermodynamics near zero temperature is that of a Fermi liquid. The case of small, but finite, dimensions is however, still open.
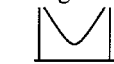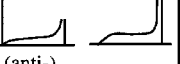
	1 d	2 d
$v_0 = v_1$ $= v_2 = v_3$ SO(4)	Luttinger Liquid spinon-holon continuum	Fermi Liquid sharp quasi-particles
$v_1 = v_2 = v_3$ $v_0 \neq v_1$ SO(3)	'Majorana Liquid' (anti-) bound-states	? ?

FIG. 12.

APPENDIX A

In this appendix, we prove by a diagrammatic method, the loop cancellation theorem for a loop with four current insertions. It is easiest to prove this in x, τ space. (For a proof in momentum-frequency space, see Kopietz et al.[24]) Let the four insertions be at $\mathbf{x}_i = (x_i, \tau_i)$, $i = 1, \ldots, 4$. Each leg of the loop is a free propagator:

$$G_{ij} \equiv G(x_i, \tau_i; x_j, \tau_j) = \frac{1}{v(\tau_i - \tau_j) + i(x_i - x_j)}.$$ (A1)

Denote by $[1234]$ the loop where, going clockwise starting from $\mathbf{x}_1$, we successively encounter $\mathbf{x}_1, \mathbf{x}_2, \mathbf{x}_3$, and $\mathbf{x}_4$, i.e.,

$$[1234] = G_{43}G_{32}G_{21}G_{14}.$$ (A2)

Without loss of generality, we can fix $\mathbf{x}_1$ and sum over permutations of the other three vertices. The loop cancellation theorem then states

$$[1234] + [1243] + [1342] + [1324] + [1423] + [1432] = 0.$$ (A3)

But for even number of propagators in a loop, going clockwise is the same as going anticlockwise; hence, e.g., $[1243] = [1342]$. Thus we only need to prove

$$[1234] + [1243] + [1324] = 0.$$ (A4)

To do this, we need the important identity

$$G_{ij}G_{jk} = G_{ik}(G_{ij} + G_{jk}),$$ (A5)

which can be proven simply by substituting in Eq. (A1). Use this to rewrite the loops

$$[1234] = G_{14}G_{43}G_{32}G_{21} = G_{13}(G_{14} + G_{43})G_{32}G_{21},$$

$$[1243] = G_{13}G_{34}G_{42}G_{21} = G_{13}(G_{34} + G_{42})G_{32}G_{21},$$

(A6)

$$[1324] = G_{14}G_{42}G_{23}G_{31} = G_{31}(G_{14} + G_{42})G_{12}G_{23},$$

and it is clear that they do all cancel, since $G_{ij} = -G_{ji}$.

From this example, we can see that it is important for the cancellation of loops with an even number of current insertions, that all the propagators be of the same type, to use identity (A5). In our context, this means all the propagators are for fermions of the same velocity.

For an odd number of insertions, identity (A5) is not needed, because time-reversal invariance guarantees the cancellation: a loop $[1ijkl \ldots xyz]$ will be canceled by the counterclockwise partner $[1zyx \ldots lkji]$, thanks to $G_{ij} = -G_{ji}$ and a total of odd number of propagators. (This is the analog of Furry's theorem in QED; see, e.g., Peskin and Schroeder.[29])

We note in passing that identity (A5) can also be used to prove the Ward identity by diagrammatic methods, order by order.[29] (For further information on the Ward identity and how it is used for diagrammatic methods for finding the exact Green function in some one-dimensional systems, see Metzner et al.[3])

APPENDIX B

Here we list some commutation relations used to derive the equations of motion of the various (classically) conserved densities. Start from the canonical anticommutation relation for the Majorana fermions:

$$\{\Psi^{(a)}(x), \Psi^{(b)}(y)\} = \delta_{ab}\delta(x-y). \quad (B1)$$

With definitions (23), and with the SO(3) Hamiltonian $H = H_0 + H_{int}$,

$$H_0 = \int dx - i\sum_{a=1}^{3} v\Psi^{(a)}(x)\partial_x\Psi^{(a)}(x)$$
$$- iv_0\Psi^{(0)}(x)\partial_x\Psi^{(0)}(x), \quad (B2)$$

$$H_{int} = -g\int dx J_{01}(x)J_{23}(x),$$

we can straightforwardly obtain

$$[J_{01}(p), H_0] = vpJ_{01}(p) + (v-v_0)K_{01}(p),$$
$$[J_{23}(p), H_0] = vpJ_{23}(p). \quad (B3)$$

We can recover SO(4) results by setting $v = v_0$. Ordinarily, we would expect $[J_{01}(p), H_{int}] = 0$, but this is spoiled by the SU(2) level-2 anomalous commutator:[30]

$$[J_{01}(p), J_{01}(q)] = [J_{23}(p), J_{23}(q)] = p\,\delta(p+q). \quad (B4)$$

One can derive this by, e.g., a diagrammatic method; see Chap. 13 of the book by Tsvelik.[30] This then leads to the only nontrivial commutation relations

$$[J_{01}(p), H_{int}] = \frac{g}{2\pi}pJ_{23}(p),$$
$$[J_{23}(p), H_{int}] = \frac{g}{2\pi}pJ_{01}(p). \quad (B5)$$

---

*Present address: Dept. of Theoretical Physics, Oxford University, 1 Keble Road, Oxford OX1 3NP, England.

[1] F. D. M. Haldane, J. Phys. C **14**, 2585 (1981).

[2] P. W. Anderson, Phys. Rev. Lett. **64**, 2306 (1990).

[3] W. Metzner and C. di Castro, Phys. Rev. B **47**, 16 107 (1993); C. di Castro and W. Metzner, Phys. Rev. Lett. **67**, 3852 (1991); W. Metzner, C. Castellani, and C. di Castro, Adv. Phys. **47**, 317 (1998), and references therein.

[4] A. Houghton and B. Marston, Phys. Rev. B **48**, 7790 (1993).

[5] A. H. Castro-Neto and E. H. Fradkin, Phys. Rev. B **51**, 4084 (1995).

[6] G. Benfatto and G. Gallavotti, Phys. Rev. B **42**, 9967 (1990).

[7] R. Shankar, Rev. Mod. Phys. **66**, 129 (1994).

[8] I. E. Dzyaloshinskii and A. I. Larkin, Zh. Éksp. Teor. Fiz. **65**, 411 (1973) [Sov. Phys. JETP **38**, 202 (1974)]. Also see H. U. Everts and H. Schulz, Solid State Commun. **15**, 1413 (1974).

[9] H.-H. Lin, L. Balents, and M. P. A. Fisher, Phys. Rev. B **56**, 6569 (1997).

[10] A somewhat less physical way to take the limit 1D→2D is to analytically continue the dimension d in calculating Feynman diagrams, akin to dimensional regularization. Again, a Fermi liquid is recovered in two dimensions; see C. Castellani, C. Di Castro, and W. Metzner, Phys. Rev. Lett. **72**, 316 (1994); and K. Ueda and T. Rice, Phys. Rev. B **29**, 1514 (1984).

[11] P. A. Bares and X. G. Wen, Phys. Rev. B **48**, 8386 (1993); Y. B. Kim et al., ibid. **50**, 17 917 (1994).

[12] P. C. E. Stamp, J. Phys. I **3**, 625 (1993).

[13] P. W. Anderson, Phys. Rev. Lett. **64**, 1839 (1990).

[14] E. Majorana, Nuovo Cimento **14**, 171 (1937).

[15] P. W. Anderson, Phys. Rev. Lett. **67**, 2092 (1991); P. Coleman, A. J. Schofield, and A. M. Tsvelik, J. Phys.: Condens. Matter **8**, 9985 (1996).

[16] V. J. Emery and S. Kivelson, Phys. Rev. B **46**, 10 812 (1992); A. M. Sengupta and A. Geroges, ibid. **49**, 10 020 (1994); P. Coleman, L. Ioffe, and A. M. Tsvelik, ibid. **52**, 6611 (1995); R. Bulla, A. C. Hewson, and G.-M. Zhang, ibid. **56**,

11 721 (1997).

[17] A. F. Ho and P. Coleman, Phys. Rev. B **58**, 4418 (1998).

[18] H. Frahm, M. P. Pfannmüller, and A. M. Tsevelik, Phys. Rev. Lett. **81**, 2116 (1998).

[19] I. Affleck, Nucl. Phys. B **265**, 409 (1986).

[20] J. F. di Tusa et al., Phys. Rev. Lett. **73**, 1857 (1994).

[21] J. D. Naud, L. P. Pryadko, and S. L. Sondhi, cond-mat/9908188 (unpublished).

[22] J. Voit, Phys. Rev. B **47**, 6740 (1993).

[23] A. F. Ho and P. Coleman, Phys. Rev. Lett. **83**, 1383 (1999).

[24] P. Kopietz, J. Hermisson, and K. Schönhammer, Phys. Rev. B **52**, 10 877 (1995).

[25] G. Baym, Phys. Rev. **127**, 1391 (1962).

[26] We used the fifth-order Runge-Kutta algorithm with adaptive stepsize control, from W. H. Press et al., *Numerical Recipes in C*, 2nd ed. (Cambridge University Press, Cambridge, 1992), Chap. 16.2. We actually solve for $1/\mathcal{G}_a$ rather than $\mathcal{G}_a$ itself, because the latter is singular and can pose problems to numerical routines.

[27] C. M. Varma et al., Phys. Rev. Lett. **63**, 1996 (1989).

[28] The SO(2)×SO(2) model can be interpreted as the low energy effective theory of the SO(4) model when an external magnetic field splits the up- and down-spin bands such that, at the Fermi energy, the bands have different slopes corresponding to the two split velocities; cf. K. Penc and J. Solyom, Phys. Rev. B **47**, 6273 (1993).

[29] For a proof of the Ward identity in QED, using diagrammatic methods analogous to ours here, see, e.g., M. E. Peskin and D. V. Schroeder, *Introduction to Quantum Field Theory* (Addison Wesley, Reading, MA, 1995).

[30] See, e.g., A. M. Tsvelik, *Quantum Field Theory in Condensed Matter Physics* (Cambridge University Press, Cambridge, 1995).

[31] Indeed, using the definitions $c_\uparrow = (1/\sqrt{2})(\Psi^{(0)} - i\Psi^{(1)})$ and $c_\downarrow = -(1/\sqrt{2})(\Psi^{(2)} + i\Psi^{(3)})$, the densities $J_{01} \propto c_\uparrow^\dagger c_\uparrow$ and $J_{23} = c_\downarrow^\dagger c_\downarrow - 1/2$ are just the spin-up and -down densities (relative

to the mean, half-filled case); hence $J_{01}+J_{23}$ is the total charge density, and $J_{01}-J_{23}$ is the spin density.

[32] This is in fact the case for the two bosonizable models mentioned here: the SO(4) model can be bosonized to a free spin boson with velocity v_{spin} and a free charge boson with v_{charge}. For the SO(2)×SO(2) model, where $v_0=v_1$ and $v_2=v_3$, this model bosonizes to two free bosons again, with velocities v_+ and v_-, as mentioned in Sec. VI.

[33] A. F. Ho and P. Coleman (unpublished).